RESEARCH AND EDUCATION

Oriented face-centered cubic to hexagonal close-packed martensitic transition, grain morphology, and mechanical properties of Co-Cr alloy fabricated by selective laser melting

Xiang Yan, MDS,[a] Ruodan Jiang, MS,[b] Wen Li, MS,[c] and Hong Lin, DDS, PhD[d]

Removable partial dentures (RPDs) have typically been made from cobalt-chromium (Co-Cr) alloys; however, the conventional lost-wax casting process for RPD frameworks is complex, and obtaining an accurately fitting prosthesis challenging.[1] Recently, selective laser melting, a metal-based 3D printing technique, has facilitated the production of RPDs with remarkable cost savings.[2-5] Co-Cr alloys are popular SLM dental materials because of their good biocompatibility, low cost, and straightforward 3D printing.[2-6] Studies have also shown that prostheses fabricated with SLM Co-Cr alloys have better corrosion resistance and higher strength compared with those fabricated with conventional casting methods.[7-9]

With the SLM process, the RPD frameworks can be printed on the metal substrate in different build orientations (Fig. 1), and the mechanical properties and

ABSTRACT

Statement of problem. Removable partial dentures (RPDs) can be fabricated by selective laser melting (SLM) with different build orientations. How microstructures and mechanical properties of SLM Co-Cr alloy are affected by different build orientations is unclear.

Purpose. The purpose of this in vitro study was to investigate the phase structures, grain morphology, and mechanical properties of SLM Co-Cr alloy with different build orientations.

Material and methods. SLM Co-Cr tensile specimens were fabricated at orientation angles of 0, 45, and 90 degrees between the building and longitudinal direction named the T0, T45, and T90 design groups (n=14). Mechanical properties were obtained by tensile testing conducted by using a universal testing machine according to the International Organization for Standardization (ISO) 22674. The grains along the longitudinal direction of the specimens and phase structures were observed before and after tensile testing by electron backscatter diffraction. One-way analysis of variance followed by the Bonferroni post hoc test and Kruskal-Wallis test were used for statistical analysis (α=.05).

Results. The 0.2% yield strengths in descending order were T90 (870 MPa)>T45 (840 MPa)>T0 (786 MPa) (P<.05); the elongations were T0 (21.8%)>T45 (15.6%)>T90 (8.7%) (P<.05); the ultimate tensile strengths were T45 (1226 MPa)>T90 (1200 MPa)>T0 (1149 MPa) (P<.05). The average grain sizes in the T0, T45, and T90 groups were 22 μm, 18 μm, and 14 μm, respectively. After the tensile test, a face-centered cubic (FCC) to hexagonal close-packed (HCP) martensitic transition was found in each group, and the phase transition area fractions were T0 (38.3%)>T45 (11.4%)>T90 (0.7%).

Conclusions. The FCC to HCP martensitic transition, grain morphology, and mechanical properties of SLM Co-Cr alloy depended on the build orientations. The oriented phase transition and grains affected the anisotropic mechanical properties of SLM Co-Cr alloy. (J Prosthet Dent 2022;127:282-7)

microstructures of the SLM Co-Cr alloys should be determined as a function of the build orientation. However, studies on this subject are sparse. Two studies have reported that the mechanical properties of the SLM

Clinical Implications

SLM Co-Cr alloys have oriented microstructures and mechanical properties that indicate SLM RPD frameworks with a specific build orientation should satisfy clinical requirements.

Co-Cr alloy depend on the build orientations,[10,11] but specific details were lacking.

The strength and ductility of Co-Cr alloys depend on the face-centered cubic (FCC) and hexagonal close-packed (HCP) crystal phases.[10,11] The FCC structure provides ductility because of easier dislocation motion; by contrast, the HCP phase is more brittle because of its limited capacity for dislocation motion.[12-14] Furthermore, the strain-induced martensitic transformation (SIMT) of the FCC phase can occur in Co-based alloys with low stacking fault energy, which can significantly affect the mechanical behavior of the alloy.[14-16] The SIMT can induce plasticity, which can increase the strength of alloys.[15,16] In addition, grain morphology can also have significant effects on the mechanical properties of alloys.[17,18]

The purpose of this in vitro study was to investigate the phase structures, grain morphology, and mechanical properties of SLM Co-Cr alloy with different build orientations. The null hypotheses were that the FCC to HCP martensitic transition, grain morphology, and mechanical properties of the SLM alloy would not depend on the build orientation.

MATERIAL AND METHODS

The Co-Cr alloy powder (Dental Co-Cr alloy powder; Upcera) with a weight percentage composition of Co 62%, Cr 25%, Mo 6%, W 5%, Si 1%, Mn 1%, Fe<1.0% was used in this study, and the particle sizes of 90% alloy powder were within 80 μm. The SLM machine (FS121M-D; Farsoon) was used to prepare the specimens under a nitrogen atmosphere; the laser spot diameter was 76 μm; the laser power was 200 W; the scan speed was 15.2 m/s; and the layer thickness was 0.03 mm. With the SLM process, the island laser scanning strategy was used as illustrated in Figure 2. As shown in Figure 3, the tensile specimens prepared in compliance with the International Organization for Standardization (ISO) 2267419 were designated according to the 0-, 45-, and 90-degree build orientations and built up with the longitudinal axes inclined from the build direction by 0-, 45-, and 90-degrees, namely the T0, T45, and T90 groups.

Fourteen specimens in each group were used for uniaxial tensile testing. The tensile testing was conducted in air at 25 °C by using a universal testing machine (3367; INSTRON) at a cross-head speed of 2 mm/min according
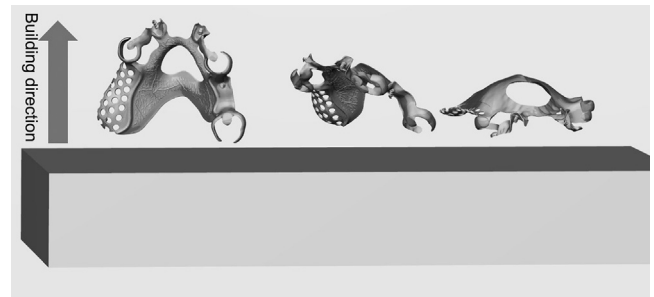

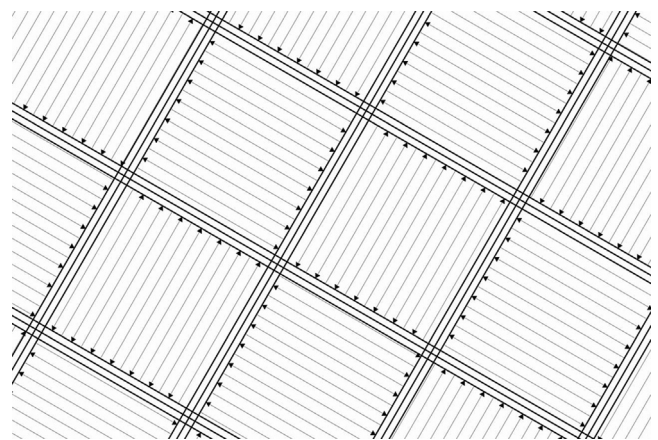**Figure 1.** Removable partial denture frameworks with different build orientations.

Figure 2. Island laser scanning strategy.

to ISO 22674.[19] The 0.2% yield strengths ($\sigma_{0.2}$) and ultimate tensile strength (UTS) were obtained from the stress-strain curves of the specimens, and the elongations were determined with the fractured pieces fitted together microscopically, which was in compliance with ISO 22674.[19]

Before and after tensile testing, 2 specimens in every group were prepared to observe the phase structure and grains by electron backscatter diffraction (EBSD). In order to prepare EBSD test specimens, cylinders with a height of 5 mm were formed by cutting along the middle of the tensile specimen before and after tensile testing. Then 1.0 mm was wet ground from the side of the cylinders by using 240-, 400-, 600-, 800-, 1000-, 1200-, and 2000-grit Al_2O_3 abrasive paper. Finally, the specimens were polished with an electrolyte consisting of glycol and sulfuric acid for Co-Cr alloy (megalyt; megadental); the electrolytic voltage was 220 V; the electrolytic current intensity was 16 A; and the electrolytic time was 8 minutes. The EBSD observations were performed in the long axis direction (Fig. 4) of the specimens before (near the center) and after the tensile test (near the specimen fracture) at a step size of 1.5 μm by using an SEM (S-3400 N; Hitachi) equipped with an EBSD system (AZtec EBSD; Oxford Instruments). Based on the EBSD technology, boundary segments with a critical orientation difference angle
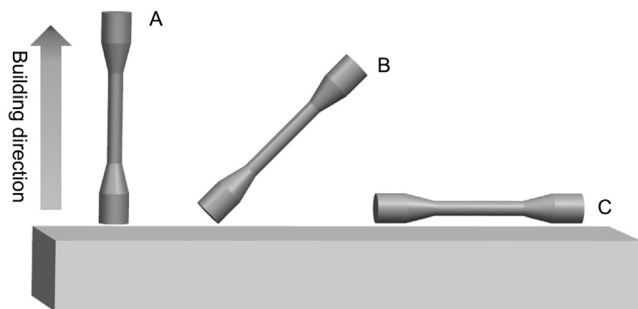
Figure 3. Selective laser melted tensile specimens with different build orientations. A, T0; B, T45; C,T90.

Figure 4. Electron backscatter diffraction observation position.

Table 1. Mechanical properties

Groups	$\sigma_{0.2}$ (MPa)	UTS (MPa)	Elongation (%)
T0	786 ±26.2	1149 ±28.1	21.8 ±3.19
T45	840 ±39.6	1226 ±26.3	15.6 ±2.66
T90	870 ±26.1	1200 ±23.7	8.7 ±1.06
T0 and T45	P<.001	P<.001	P<.001
T0 and T90	P<.001	P<.001	P<.001
T45 and T90	P=.046	P=.035	P<.001

$\sigma_{0.2}$, 0.2% yield strength; UTS, ultimate tensile strength.

higher than 10 degrees were identified and defined as grain boundaries. The EBSD data were collected and analyzed by using a software package (HKL Channel 5; Oxford Instruments). The experimental data were evaluated with 1-way analysis of variance (ANOVA) followed by the Bonferroni post hoc test with a statistical software program (IBM SPSS Statistics, v24.0; IBM Corp) and the Kruskal-Wallis test (α=.05).

RESULTS

As can be seen from Table 1, the order from the highest to lowest $\sigma_{0.2}$ values of the test specimens was T90>T45>T0. The variability of $\sigma_{0.2}$ values among the 3 groups was homogeneous ($df1$=2; $df2$=39; P=.221). One-way ANOVA analysis revealed a significant difference in the $\sigma_{0.2}$ ($df1$=2; F=25.823; P<.05), and the Bonferroni post hoc test demonstrated significant differences among the groups (P<.05). The order of the UTS values was T45>T90>T0. As a result of homogeneous variability ($df1$=2; $df2$=39; P=.137), the 1-way ANOVA analysis revealed a significant difference in the UTS results in the 3 groups ($df1$=2; F=31.661; P<.05), and the Bonferroni post hoc test showed significant differences among the groups (P<.05). The elongation values were T0>T45>T90, while the variability among the 3 groups was inhomogeneous ($df1$=2; $df2$=39; P<.001). The Kruskal-Wallis test showed significant differences in the elongation values among the groups (P<.05).

Figure 5 shows the grain morphologies and low-angle grain boundaries (LAGBs, <15 degrees), where it can be seen that the long axis of the grains and grain boundaries of T0 and T45 were the same as the corresponding build orientations. In addition, the grain overall morphology of T90 was similar for different scanning strategies. The mean values and standard deviations of the grain sizes in the T0, T45, and T90 groups were 22 ±23 µm, 18 ±16 µm, and 14 ±12 µm, respectively. Moreover, group T90 showed that the LAGBs were mainly located in the crisscrossing regions of the island laser scanning strategy, where the grain sizes were smaller. Compared with T0 and T45, the LAGBs of T90 were denser.
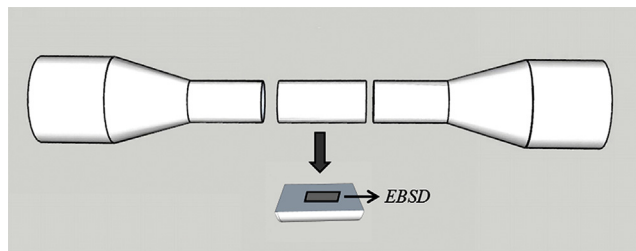
The EBSD phase map (Fig. 6) indicates that the tested regions of the specimens before the tensile test consisted of a single FCC phase without an HCP phase. However, after the tensile test, the HCP phase was found in all of the specimens, and in the order from the highest to lowest HCP phase area fractions in tested regions of the specimens were T0 (38.3%)>T45(11.4%)>T90 (0.7%). These indicated that the FCC to HCP martensitic transformation occurred during the tensile test. In addition, the HCP phase texture direction of T0 and T45 were identical to the corresponding build orientation.

DISCUSSION

The ductility and strength of the SLM Co-Cr alloys tested depended on the build orientation and exceeded the requirements of ISO 22674[19] for the V type alloy ($\sigma_{0.2}$ ≥500 MPa, elongation ≥2 %) used for thin metal RPD, frameworks. Furthermore, clear distinctions were found in the grain morphology and FCC to HCP transformation in the T0, T45, and T90 groups. Therefore, the null hypothesis was rejected.

Variations in grain shapes among the 3 groups were clear in the microscopic observations (Fig. 5). Because of the directional solidification during the SLM process, the grains of the T0 and T45 groups extended and stacked along the build orientations, creating aligned grain structures and larger grain sizes than T90 along the build orientations. The tested surface of T90 was perpendicular to the build direction, and its grain overall morphology was similar to islands or a chessboard, reflecting the characteristics of the scanning strategy. When the direction of shear stress is consistent with or close to the grain boundary, the probability of dislocation blocking
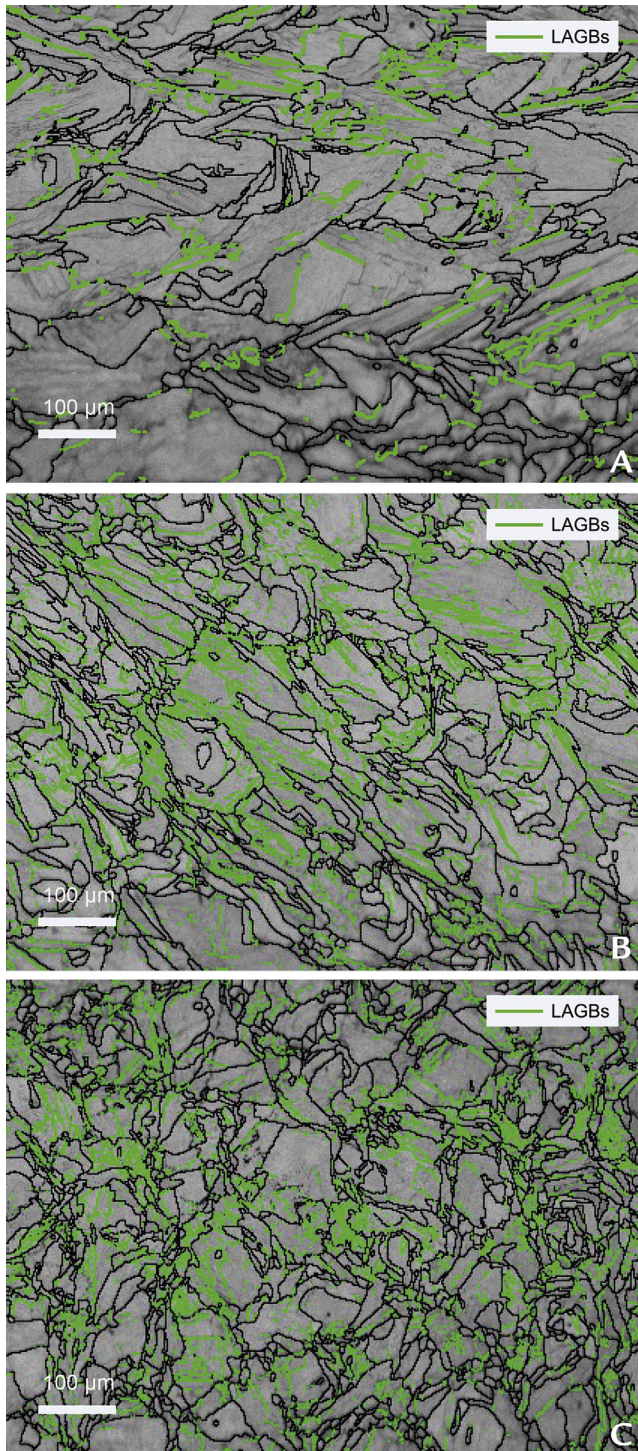
Figure 5. Grain morphologies. A, T0; B,T45; C, T90. Original magnification ×250. LAGBs, low-angle grain boundaries (LAGBs, <15 degrees)

has been reported to decrease, resulting in lower yield strength.[17] In the present study, the order of largest to smallest grain size was T0>T45>T90; however, these grains were observed on 2D surfaces of specimens, mainly reflecting the 2D dimensions of grains in the build

orientation and the 3D dimensions of theses grains were unclear. The LAGBs pose a major obstacle to dislocation penetration, and the interaction of dislocations with LAGBs has been shown as a substantial contribution to the strength of metals.[20,21] Therefore, the differences of LAGBs in the 3 groups should also contribute to the differences of their yield strengths.

The FCC phase is stable at high temperatures, while the HCP phase exists as an equilibrium phase at lower temperatures.[13,16,22] The equilibrium phase diagram of Co-Cr alloys indicates that at >900 °C, the expected structure is the FCC structure and that at <900 °C, it is the HCP structure.[23-25] Under the thermodynamic conditions of below or about 900 °C, accompanied by the diffusion of alloy elements, the diffusional FCC to HCP martensitic transformation occurs slowly in Co-Cr alloy.[23-25] In addition, because of a low stacking fault energy, the FCC to HCP martensitic transformation during plastic deformation at room temperature also occurs because of shear of $1/6 <1\bar{2}10>$ on $\{111\}_{fcc}$ planes, referred to as the SIMT.[14-16,26]

With the SLM process, rapid cooling of the specimen suppresses the FCC to HCP transition; consequently, the FCC structure is dominant in the as-built SLM Co-Cr alloy.[10,11,23,24,27] After the tensile test, the HCP structure was present, which indicated that the SIMT with FCC to HCP transformation occurred during the tensile test. Furthermore, this induced martensitic transformation can also increase plasticity.[28] Under tensile stress, the FCC to HCP transformation causes stress relaxation in the specimen and gives rise to a uniform deformation in the SLM Co-Cr alloy instead of necking behavior, which leads to high UTS and high plasticity.[28] In the present study, the FCC to HCP transformation of the SLM Co-Cr alloy depended on the build orientation, and the experimental results revealed that the area percentages of FCC to HCP transformation in the tested area of T0, T45, and T90 were 38.3%, 11.4%, and 0.7%, respectively. Therefore, in the order of highest to lowest ductility, the specimens were T0>T45>T90. Furthermore, the yield strengths of T45 were lower than those of T90, but it had higher ultimate tensile strengths, which may be attributed to this phase transition. During the FCC to HCP transition, the 2 structures should follow the orientation relationship of $\{111\}_{fcc} \| \{0001\}_{hcp}$ based on the gliding of the partial dislocation of $1/6 <1\bar{2}10>$ in every second $\{111\}_{fcc}$ plane.[14-16,26] The orientation relationship probably resulted in the phase transformation of SLM Co-Cr alloy depending on the build orientation; however, the mechanism should be further studied.

Cast Co-Cr alloy typically exhibits isotropic microstructures and mechanical properties. However, casting defects such as pores are unavoidable and reduce the ductility and strength of dental Co-Cr RPD frameworks. The present study highlights that the microstructures of
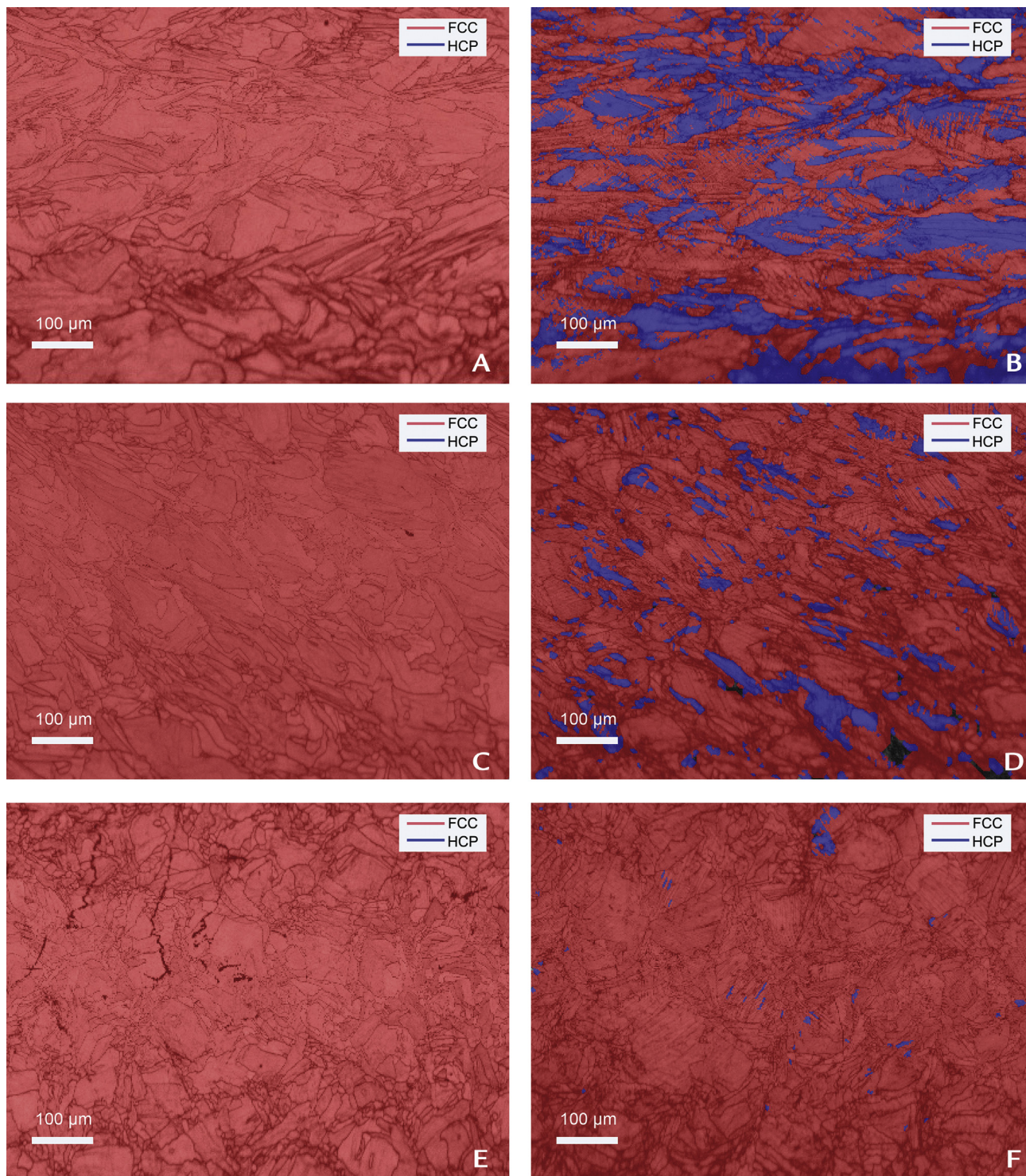
Figure 6. Phase structures. A, T0; B, T0 after tensile test.; C, T45; D, T45 after tensile test; E, T90; F, T90 after tensile test. Original magnification ×250. FCC, face-centered cubic; HCP, hexagonal close-packed.

the Co-Cr alloy fabricated using SLM have unique grain morphologies and FCC to HCP phase transformation, thereby improving the ductility and strength of the alloy. In addition, the differences between the mechanical properties and microstructure of SLM Co-Cr alloy restorations with different build orientations require increased attention that can lead to further understanding when SLM Co-Cr frameworks are used in clinical applications. SLM Co-Cr alloys have oriented microstructures and mechanical properties indicating that the

RPD framework with a specific build orientation should satisfy clinical requirements. Currently, there is no ISO standard for dental metal materials used for 3D printing technology and 3D-printed metal prostheses. Therefore, the results of this study suggest that the build orientation should be considered when relevant standards are drafted.

Residual stresses occur in the SLM process, which may result in the deformation of moldings so that heat treatment of the part is necessary to relieve the stress after the parts are printed.[2,29] Therefore, based on this study, further work should identify suitable heat treatments and determine whether heat treatments can eliminate the differences of mechanical behavior and microstructure in the SLM Co-Cr parts with different build orientations.

CONCLUSIONS

Based on the findings of this in vitro study, the following conclusions were drawn:

1. The FCC to HCP martensitic transition, grain morphology, and mechanical properties of the SLM Co-Cr alloy depended on the build orientation.
2. The oriented FCC to HCP phase transition and grain morphology influenced the anisotropic mechanical properties of SLM Co-Cr alloy.

REFERENCES

1. Zhou XS, Tong D. Prosthodontic technology. 1st ed. Beijing: Peking University Medical Press; 2014. p. 307.
2. Yan X, Lin H, Wu Y, Bai W. Effect of two heat treatments on mechanical properties of selective-laser-melted Co-Cr metal-ceramic alloys for application in thin removable partial dentures. J Prosthet Dent 2018;119:1028.e1-6.
3. Øilo M, Nesse H, Lundberg OJ. Mechanical properties of cobalt-chromium 3-unit fixed dental prostheses fabricated by casting, milling, and additive manufacturing. J Prosthet Dent 2018;120:156.e1-7.
4. Alifuisegbaya F, Williams JR, George R. Additive manufacturing: a novel method for fabricating cobalt-chromium removable partial denture frameworks. Eur J Prosthodont Restor Dent 2017;25:73-8.
5. Braian M, Jönsson D, Kevci M, Wennerberg A. Geometrical accuracy of metallic objects produced with additive or subtractive manufacturing: a comparative in vitro study. Dent Mater 2018;34:978-93.
6. Kim E, Lee D, Kwon S, Kwon T. A microcomputed tomography evaluation of the marginal fit of cobalt-chromium alloy copings fabricated by new manufacturing techniques and alloy systems. J Prosthet Dent 2016;117:393-9.
7. Lu Y, Wu S, Gan Y, Li J, Zhao C. Investigation on the microstructure, mechanical property and corrosion behavior of the selective laser melted CoCrW alloy for dental application. Mater Sci Eng C Mater Biol Appl 2015;49:517-25.
8. Wang WJ, Yung KC, Choy HS, Xiao TY, Cai ZX. Effects of laser polishing on surface microstructure and corrosion resistance of additive manufactured CoCr alloys. Appl Surf Sci 2018;443:167-75.
9. Zeng L, Xiang N, Wei B. A comparison of corrosion resistance of cobalt chromium molybdenum metal ceramic alloy fabricated with selective laser melting and traditional processing. J Prosthet Dent 2014;112:1217-24.
10. Takaichi A, Suyalatu, Nakamoto T, Joko N, Nomura N. Microstructures and mechanical properties of Co-29Cr-6Mo alloy fabricated by selective laser melting process for dental applications. J Mech Behav Biomed Mater 2013;21:67-76.
11. Kajima Y, Takaichi A, Nakamoto T, Kimura, Yoqo Y. Fatigue strength of Co-Cr-Mo alloy clasps prepared by selective laser melting. J Mech Behav Biomed Mater 2016;59:446-58.
12. Allan FC, Asgar K. Reaction of cobalt-chromium casting alloy with investment. J Dent Res 1966;45:1516-28.
13. Yamanaka K, Mori M, Chiba A. Nanoarchitectured Co-Cr-Mo orthopedic implant alloys: nitrogen-enhanced nanostructural evolution and its effect on phase stability. Acta Biomater 2013;9:6259-67.
14. Mittemeijer EJ. Fundamentals of materials science. 1st ed. Berlin: Springer; 2010. p. 107-228.
15. Mani A, Rodriguez S, Lopez HF. Deformation induced FCC to HCP transformation in a Co-27Cr-5Mo-0.05C alloy. Mater Sci Eng A 2011;528:3037-43.
16. Mitsunobu T, Koizumi Y, Lee BS, Yamanaka K, Matsumota H, Li Y, et al. Role of strain-induced martensitic transformation on extrusion and intrusion formation during fatigue deformation of biomedical Co-Cr-Mo-N alloys. Acta Mater 2014;81:377-85.
17. Cho KK, Chung YH, Lee CW, Kwun SI, Shin MC. Effects of grain shape and texture on the yield strength anisotropy of Al-Li alloy. Scr Mater 1999;40:651-7.
18. Christian JW. The theory of transformations in metals and alloys. 3rd ed. St. Louis: Elsevier; 2002. p. 961-1075.
19. International Organization for Standardization. ISO 22674. Dentistry -metallic materials for fixed and removable restorations and appliances. Geneva: International Organization for Standardization; 2016. Available at: https://www.iso.org/standard/59620.html.
20. Liu B, Raabe D D, Eisenlohr P, Roters F, Arsenlis A, Hommes G. Dislocation interactions and low-angle grain boundary strengthening. Acta Mater 2011;59:7125-34.
21. Liu B, Eisenlohr P, Roters F, Raabe D. Simulation of dislocation penetration through a general low-angle grain boundary. Acta Mater 2012;60:5380-90.
22. Veprek S. The search for novel superhard materials. J Vac Sci Technol A 1999;17:2401-20.
23. Li KC, Prior DJ, Waddell JN. Comparison of the microstructure and phase stability of as-cast, CAD/CAM and powder metallurgy manufactured Co-Cr dental alloys. Dent Mater 2015;31:e306-15.
24. Li KC, Tran LY, Prior DJ. Porcelain bonding to novel Co-Cr alloys: influence of interfacial reactions on phase stability, plasticity and adhesion. Dent Mater 2016;32:1504-12.
25. Yan X, Xu YX, Wu Y. Effects of heat treatment on metal-ceramic combination of selective-laser-melted cobalt-chromium alloy. J Prosthet Dent 2018;120:319.e1-6.
26. Koizumi Y, Suzuki S, Yamanaka K. Strain-induced martensitic transformation near twin boundaries in a biomedical Co-Cr-Mo alloy with negative stacking fault energy. Acta Mater 2013;61:1648-61.
27. Zhou YN, Li N, Yan JZ. Comparative analysis of the microstructures and mechanical properties of Co-Cr dental alloys fabricated by different methods. J Prosthet Dent 2018;120:617-23.
28. Cooman BC. Structure-properties relationship in TRIP steels containing carbide-free bainite. Curr Opin Solid St M 2004;8:285-303.
29. Li C, Liua JF, Fang XF, Guoa YB. Efficient predictive model of part distortion and residual stress in selective laser melting. Addit Manuf 2017;17:157-68.

Corresponding author:
Dr Hong Lin
22 Zhongguancun Avenue South
Haidian District, Beijing 100081
PR CHINA
Email: linhong195@163.com

CRediT authorship contribution statement
Xiang Yan: Conceptualization, Methodology, Validation, Formal analysis, Investigation, Data curation, Writing - original draft, Writing - review & editing. **Ruodan Jiang:** Investigation, Data curation, Formal analysis. **Wen Li:** Validation, Investigation, Data curation. **Hong Lin:** Conceptualization, Writing - review & editing, Supervision, Project administration, Funding acquisition.